DESIGN AND PERFORMANCE ANALYSIS OF EXPANDER FOR WASTE HEAT RECOVERY APPLICATION

Tee Jia Zheng[a], Chiong Meng Soon[b*], Mahadhir Mohammad[b], Chun Mein Soon[b]

[a] Faculty of Mechanical Engineering, Universiti Teknologi Malaysia, 81310 UTM Johor Bahru, Johor, Malaysia
[b] UTM LoCARtic, Institute for Sustainable Transport (IST), Universiti Teknologi Malaysia, 81310 UTM Johor Bahru, Johor, Malaysia

Article history
Received
7th November 2024
Received in revised form
8th December 2024
Accepted
8th December 2024
Published
26th December 2024

*Corresponding author
chiongms@utm.my

GRAPHICAL ABSTRACT

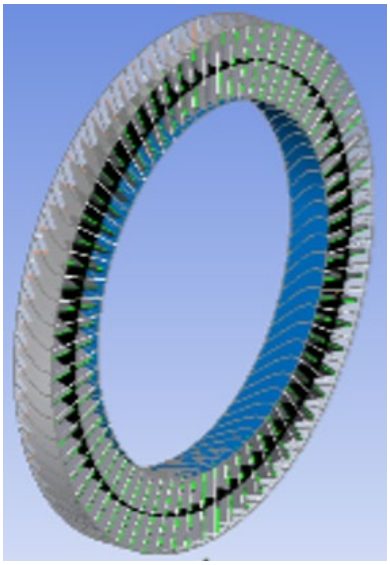

ABSTRACT

Waste heat recovery (WHR) is one of the solutions for net zero carbon and decarbonization activity. Currently, the Organic Rankine Cycle is widely studied because of its capability to operate at a wide range of temperatures, scalability, lower operating temperature, and high thermal efficiency. Despite advancements, challenges in expander design and performance analysis limit waste heat recovery. Therefore, the objective is to design and analyse a suitable expander for waste heat recovery and achieve a total-to-total efficiency exceeding 70% with a minimum power output of 30kW at a pressure ratio of 1.4. The design and performance analysis for 3D blade geometry and expander using the ANSYS CFX software. An applied meanline modelling was conducted using MATLAB. The results demonstrated the expander's capability to generate 35.857 kW of power, exceeding the design target. Additionally, a total-to-total efficiency of 74.69% was achieved, surpassing the minimum efficiency threshold of 70%, even after accounting for tip leakage losses. The findings contribute valuable insights for optimizing expander designs and advancing waste heat recovery technologies aligning with global efforts to promote sustainable energy systems.

KEYWORDS

Axial Expander; Meanline Approach; Computational Fluid Dynamics ANSYS CFX; Waste Heat Recovery

INTRODUCTION

In recent decades, human dependency on energy and environmental issues has increased. Global oil consumption, reaching about 76 million barrels per day, has resulted in challenges such as climate change and ozone layer depletion [1]. To address these issues, two main approaches have emerged: reducing reliance on non-renewable energy and improving energy conversion systems.

While turbines are highly efficient for waste heat recovery in power generation at the MW level, their efficiency decreases at smaller scales. Thus, for lower power generation in the 1kW

to 10kW range, replacing turbines with displacement expanders is preferable. Expanders are expansion machines that increase volume by decreasing fluid pressure. They consist of a stator, rotor(s), and an expander shaft. The high-pressure working fluid, like refrigerant R123 or R717, causes the rotor to rotate, converting fluid energy into mechanical motion and generating shaft work.

This research work aims to design, study, and determine the appropriate type of expander for waste heat recovery, considering specific conditions such as pressure ratio, temperature, and output power. It also involves developing a simulation model for axial expander design, analysing geometry, thermodynamic states, and performance in waste heat recovery applications.

Working Fluid

The choice of working fluid is critical for cycle efficiency and waste heat recovery applications, as it significantly impacts the performance of the expander in waste heat recovery systems. Fluids with low Global Warming Potential (GWP) and Ozone Depletion Potential (ODP) are generally prioritized [2–4]. A case study titled "A Performance Study of R717 and R22 As the Working Fluid for OTEC Plant" indicates that R717 is a refrigerant with a GWP of zero, making it environmentally friendly. Consequently, R717 has been selected as the working fluid for this study [5].

Expansion Devices

Although large-scale expanders have seen development, the maturity of small-scale expanders in the market is still low. Therefore, significant research and development (R&D) activities are necessary to meet the requirements of Organic Rankine Cycle (ORC) systems. In general, the selection of a suitable expander is dominant and vital for waste heat recovery application and power generation. This is because the expander is a vital device in an efficient and cost-effective ORC system. There are different types of expansion devices that can be used in small-power ORC systems which rely on operating conditions such as working fluid, temperature, and mass flow rate. Not only that, when selecting the expander, criteria such as high isentropic efficiency, pressure ratio, and power output should be considered [6, 7]. The expansion machines can be divided into two groups which are the volumetric expander (Positive Displacement Expander) and dynamic expander (Turbo-expander) which are shown in Figure 1.

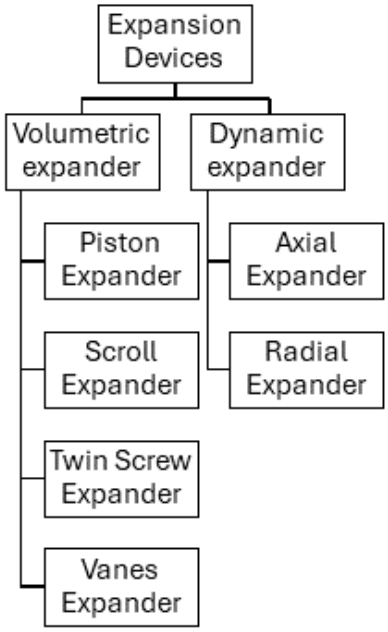

Figure 1: Classification of expansion devices [8]

Selection Criteria of Expander

One of the primary criteria to consider when selecting an expansion device is the range of power it can produce. As shown in Figure 2, twin screw expanders and dynamic expanders are typically recommended for applications requiring more than 10 kW of power. For applications with power outputs below 10 kW, scroll and piston expanders may be suitable alternatives [9].

Besides the power range, other technical limitations such as pressure ratio and manufacturing cost should be considered. Based on Figure 3, the twin screw expander is unable to operate under a low-pressure ratio of 1.4 and the isentropic efficiency is the lowest among the expanders.

Cost efficiency is a crucial factor for designers when selecting a suitable expander. Figure 4 illustrates that the manufacturing cost per unit of power output is highest for radial expanders, followed by twin screw expanders, axial expanders, piston expanders, scroll expanders, and vane expanders. Therefore, when choosing an expander, it is essential to consider the power output range, pressure ratio, and cost efficiency [10].

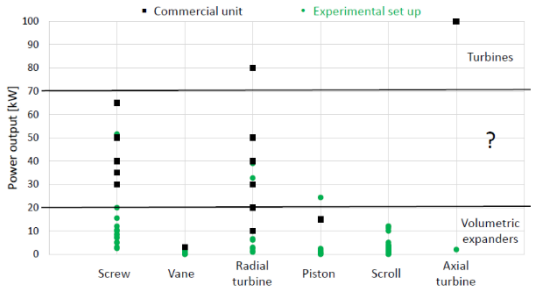

Figure 2: Ranges of power produced by expanders [11]

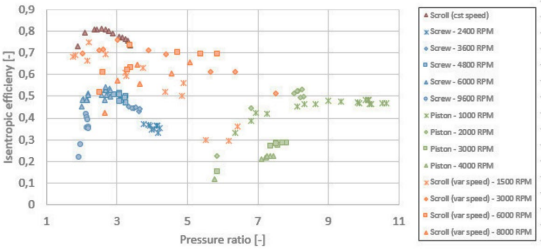

Figure 3: Isentropic efficiency versus pressure ratio for each expander [12]

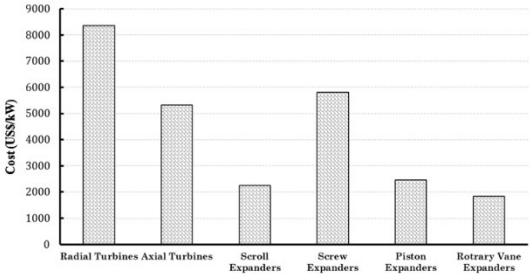

Figure 4: Cost estimation of expanders based on power output for each expander [13]

METHODOLOGY

A detailed overview of the essential design parameters, the geometry, and the prediction of expander performance were introduced. The process of developing the axial turbine included: one-dimensional mean-line modelling was initially followed, then the calculation of the blade geometry and losses evaluation. To further analyse and refine the design, computational fluid dynamics (CFD) simulations were employed using ANSYS.

Meanline Expander Design Approach

The meanline model assumes that the flow parameters at the mean radius of the flow passage can accurately represent the average values of the entire cross-section, disregarding variations in parameters along the radial and circumferential directions. The purpose of the meanline model is to establish the overall geometry of the axial expander and the initial performance parameters. This approach allows for estimating output power and turbine efficiency based on performance and loss estimations under various operating conditions.

Figure 5 shows the overall process of the meanline modelling code flow chart. The given parameters for a meanline design vary from one application to another, but in general, it comprises inlet total pressure and temperature, the mass flow rate of the working fluid, pressure ratio, non-dimension parameters, rotational speed, output power, and targeted efficiency.

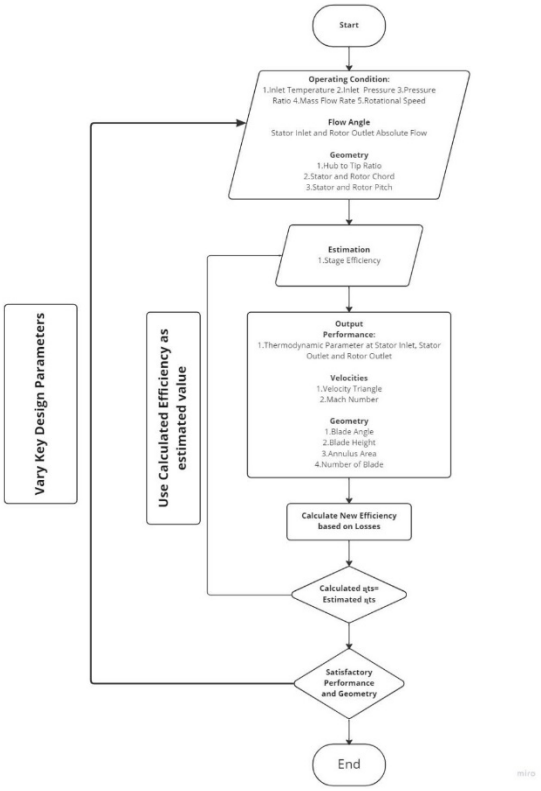

Figure 5: Meanline modelling code flow chart

Meanline Calculation Through MATLAB

To keep the preliminary design of the axial turbine realistic, a mathematical iteration calculation method is used in mean line analysis. Firstly, a set of limitations will be imposed on various design parameters. For instance, a negative swirl at the exit from the rotor is beneficial in improving the work output, allowing for a permissible exit flow angle of -15°. In addition, larger values of exit flow angle should be avoided since it might limit the off-design operation of the stage [1].

Next, the relative Mach number at the rotor exit and the absolute Mach number at the exit from the stator at the mean radius are limited to 0.95. Although this will indicate that the Mach number at the turbine blade tip could be slightly transonic, it is highly improbable that it would reach

excessively high levels. The turbine inlet temperature is set at 298K, and discharge pressure is set at 700 Pa, a desired pressure at the turbine outlet. The speed of rotation for the turbine is determined based on the requirements of matching with other components, and it is set to 8500 rpm. This speed ensures compatibility and proper functioning of the axial turbine in conjunction with other system components. The working fluid of this analysis is R717 and it is assumed to behave as vapor liquid. The specific heat ratio is determined to be 1.473 for this refrigerant.

Moreover, it is important to verify that the value of the stator exit temperature obtained in the previous step aligns with the specified turbine inlet temperature since there is no change in total temperature across the stator (assuming adiabatic flow). The iterated variable is the rotor exit static temperature initially estimated at the start of the step in the Rotor Exit. Closure can be obtained quite quickly since the iteration is a very trivial process. Once the iteration is complete, the stage calculations are finalized. At this stage, the turbine's performance can be established, and the remaining gas flow angles can be calculated. These calculations are essential for understanding the flow behaviour and optimizing the turbine's efficiency.

$$\text{Power} = \text{m}\Delta\text{UC}_\theta \quad \text{Eq.1}$$

$$\text{m} = \rho_3 \text{A}_3 \text{C}_{\text{m}3} \quad \text{Eq.2}$$

$$\psi = \frac{\text{C}_\text{p}(\text{T}_{02} - \text{T}_{03})}{\text{U}^2} \quad \text{Eq.3}$$

$$ø = \frac{\text{C}_{\text{m}3}}{\text{U}} \quad \text{Eq.4}$$

$$\alpha_2 = \tan^{-1}\left(\frac{\text{C}_{\theta 3}}{\text{C}_{\text{m}3}}\right) \quad \text{Eq.5}$$

$$\beta_2 = \tan^{-1}\left(\frac{\text{U} - \text{C}_{\theta 2}}{\text{C}_{\text{m}2}}\right) \quad \text{Eq.6}$$

$$\beta_3 = \tan^{-1}\left(\frac{\text{U} - \text{C}_{\theta 3}}{\text{C}_{\text{m}3}}\right) \quad \text{Eq.7}$$

At this stage of the analysis, it is beneficial to assess the overall feasibility of the turbine stage from practical aerodynamic perspectives. Useful checks are to construct the velocity triangles and plot the blade loading and flow coefficients respectively, on the Smith chart which is shown in Figure 6 and Figure 7. If the blade loading and flow coefficients fall within acceptable ranges, it indicates that the predicted operation of the turbine stage is reasonable. From these, it may be reasonably concluded that the predicted operation and velocity triangles are all quite acceptable and that the related stage can be successfully built.

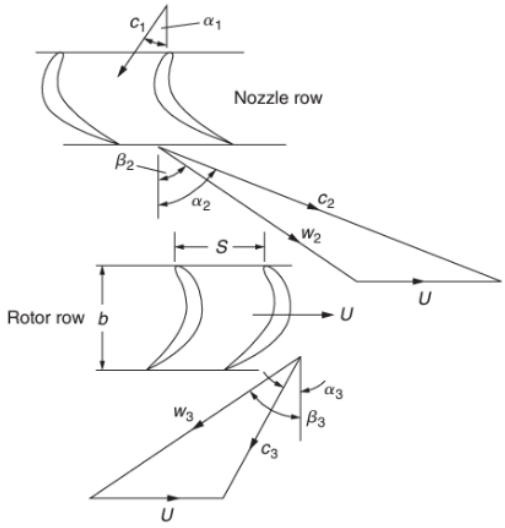

Figure 6: Rerated stage velocity triangles [14].

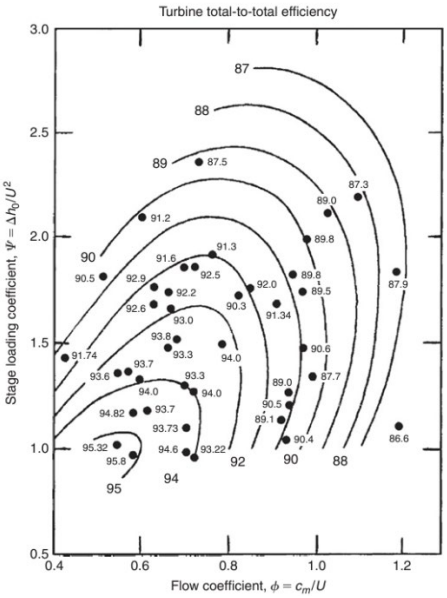

Figure 7: Rerated stage performance plotted on Smith Chart [14].

CFD Axial Expander Modelling

CFD simulations involve solving the partial differential equations (Navier-Stokes N-S) that govern the flow field using numerical methods such as finite difference and finite volume approaches.

With CFD, turbines can be modelled with single or multiple stages, and both steady-state and transient flow conditions can be considered. By using CFD, the designer can gain a deeper understanding of the complex flow through the turbine passages. Studying the impact of geometry variations on overall performance in terms of power and torque produced, total-to-total efficiency and total-to-static efficiency allows for the refinement and improvement of expander

design. This section will explain the theory of CFD modelling as a powerful numerical tool for designing the axial expander.

CFD Axial Turbine Modelling Using Ansys CFX

The primary objective of turbine CFD modelling is to improve the output of 1D mean line design by simulating the preliminary design. With CFD simulations, an expander performance in terms of power output, torque, total-to-total efficiency, and total-to-static efficiency can be generated based on the targeted operating conditions when the pressure ratio is 1.42, initial temperature is 25℃ and R717 as the working fluid. In this research, a 3D CFD simulation of an axial expander was conducted using ANSYS CFX. Figure 8 indicates the general procedure for CFD modelling of the axial expander using ANSYS and overall procedures of CFD simulation using ANSYS Turbomachinery Package respectively [1].

First and foremost, the detailed geometry for both stator and rotor blades was defined using CFX-BladeGen. Once the blade geometry was established, the fluid domain was discretised into cells using CFX TurboGrid. The flow was then solved as a 3D steady, compressible, and adiabatic flow using the CFX solver. This section provides an overview of the methodology employed for axial expander CFD modelling using ANSYS CFX [15].

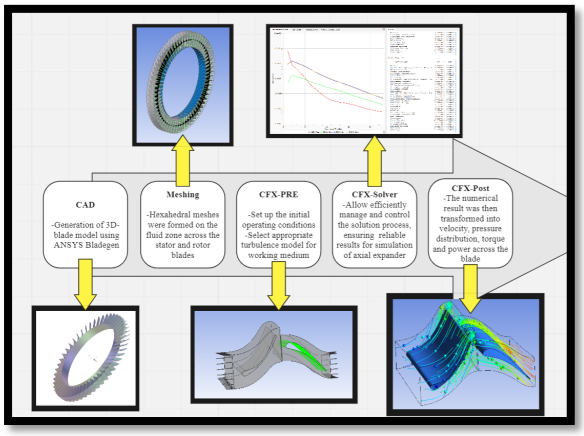

Figure 8: Overall procedures of CFD simulation using ANSYS Turbomachinery Package

Results and Discussions

This section describes the results of the study carried out to develop a small-scale axial expander using 1D meanline modelling as described in the methodology section. The purpose of this study is to design an axial expander for a specific set of operating conditions. The target operating parameters include a pressure ratio of 1.42, an inlet temperature of 298K, and the utilization of R717 as the working fluid. The research goal is to achieve a desired power output of 30kW from the axial expander.

Velocity Triangle

The flow coefficient, stage loading, and degree of reaction were utilized in a 1D modelling process. This helped in determining the expander velocity triangles and calculating the thermodynamic properties of the working fluid at the mean-line. By using velocity triangles, all velocity components, and absolute and relative blade angles can be calculated. The shape of velocity triangles is influenced by three non-dimensional design parameters which include the degree of reaction, the flow coefficient, and the stage loading coefficient [16]. Hence, the flow development in the axial turbine stage (stator and rotor) can be described by velocity triangles at the expander blade mean diameter as shown in Figure 9.

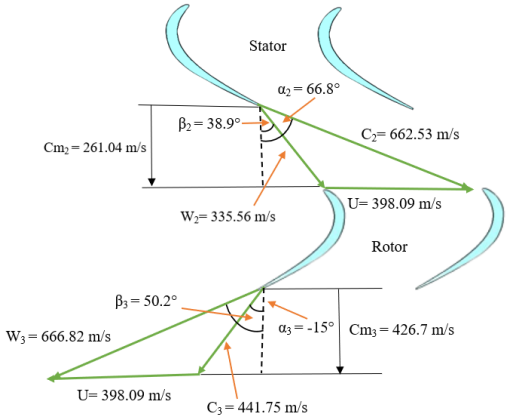

Figure 9: Rerated stage velocity triangles for designed axial expander

Smith Chart Prediction

Since the blade loading and flow coefficients fall within acceptable ranges, it indicates that the predicted operation of the expander stage is reasonable when the values of flow coefficient, ø, and stage loading coefficient, ψ are 1.0719 and 1.8168 respectively. Based on the smith chart shown in Figure 10 it indicates that the total-to-total efficiency is nearly equal to 89%.

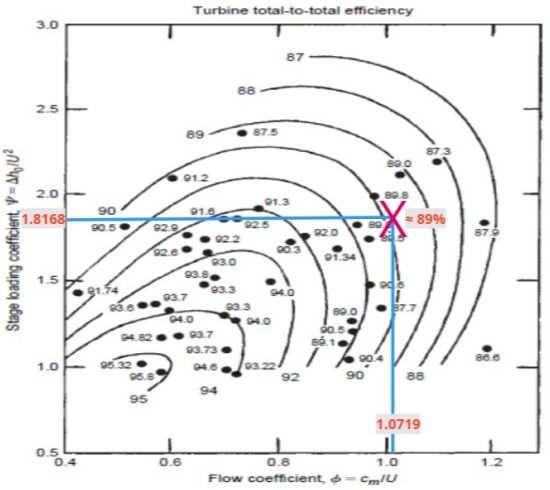

Figure 10: Smith chart prediction for preliminary designed axial expander

Meanline Modelling Results

Based on Table 1, indicates that the total-to-total efficiency of the meanline results is 74.69% which is lower than the efficiency expected from the Smith chart by 14.31%. This is because the efficiency values of the meanline approach are corrected to eliminate the effects of tip leakage. Also, the Smith chart is a generalized correlation of turbine data which has proved to be valuable in indicating trends in expander performance because of overall design parameters, but it cannot be expected to give completely realistic values of efficiency in every design.

Table 1: Axial expander preliminary design modelling results

Selected Parameter	Unit	Value
Expander Output power	kW	35.857
Total-to-Static Efficiency	%	34.19
Total-to-Total Efficiency	%	74.69

In addition, the low total-to-static efficiency can be attributed to several factors, including irreversible losses. These losses occur due to various factors such as fluid friction, shock waves, and boundary layer separation. These losses result in a decrease in the total pressure and energy of the fluid, leading to a lower total-to-static efficiency.

3D CFD Simulation Results

The CFD simulation results are presented using velocity vectors, Mach number contours, and blade loading distributions at specific blade spans. The first figure depicts velocity vectors through the axial expander stage at 50% blade span, while the second figure illustrates velocity vectors at 90% blade span. Both figures indicate limited flow separation and vortices on the rotor blade suction side near the trailing edge region. These vortices can lead to energy losses within the expander, causing turbulence, pressure drops, and flow separation, which in turn increase fluid resistance and reduce overall expander efficiency. However, the observed flow behaviour suggests that the blade profile considering blade thickness distribution and flow turning angle can be characterized as a well-designed aerodynamic profile, minimizing such inefficiencies effectively.

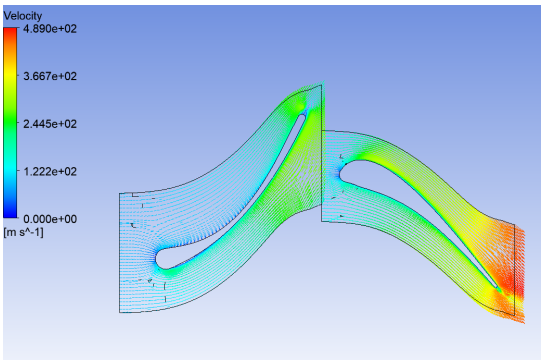

Figure 11: Velocity vectors through axial expander stage for 50% blade span

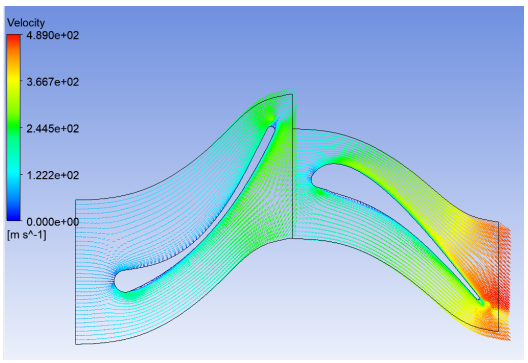

Figure 12: Velocity vectors through axial expander stage for 90% blade span

Comparison Between 1D Meanline Modelling and 3D CFD Simulation Results

A detailed comparison between 1D meanline modelling and 3D CFD simulations is provided in Table 2. To improve the expander blade's aerodynamic performance as the flow moves from the stator to the rotor blades, the blade profile was modified to reduce secondary flow regions and flow separation at the leading and trailing edges.

Table 2: Comparison between 1D meanline modelling and 3D CFD simulations

Parameter	1D Meanline Results	CFD Simulation Results	Deviation
T_{01} (K)	298	298	0
P_{01} (Pa)	1000	1000	0
P_3 (Pa)	700	716.296	16.296
$\dot{m}_{R717}$ (kg/s)	0.448	0.448	0
Power output (kW)	35.857	32.766	3.091
Total-to-static efficiency (%)	34.19	28.93	5.26
Total-to-total efficiency (%)	74.69	69.99	4.7

Based on Table 2, there are some deviations in terms of outlet pressure of the rotor blade, output power generated, total-to-static efficiency, and total-to-total efficiency. This is because the choice of the isentropic equation used in meanline analysis can impact the power and efficiency calculations, particularly when the working fluid deviates from the ideal gas assumption. Despite the deviation, the meanline model is still chosen because of its practicality and computational efficiency. Meanline analysis often relies on simplified isentropic equations that assume ideal gas behaviour, which may not accurately capture the thermodynamic properties of non-ideal working fluids like R717.

Conclusion

The designed axial expander surpassed the objective by generating 35.857 kW of power and achieving a total-to-total efficiency of 74.69%, exceeding the minimum efficiency requirement of 70%. This validates its potential for effective waste heat recovery, contributing to energy efficiency and environmental sustainability.

Acknowledgements

The authors would like to express their appreciation for the support of the Ministry of Higher Education Malaysia (MoHE) for the funding of this research under the registered program cost center #R.J130000.7851.4L893.

References

[1] Mahmoudi A, Fazli M, Morad MR. A recent review of waste heat recovery by Organic Rankine Cycle. *Applied Thermal Engineering* 2018; 143: 660–675.

[2] Le VL, Feidt M, Kheiri A, et al. Performance optimization of low-temperature power generation by supercritical ORCs (organic Rankine cycles) using low GWP (global warming potential) working fluids. *Energy* 2014; 67: 513–526.

[3] Bahrami M, Pourfayaz F, Kasaeian A. Low global warming potential (GWP) working fluids (WFs) for Organic Rankine Cycle (ORC) applications. *Energy Reports* 2022; 8: 2976–2988.

[4] Zhang Y, Yang K, Li X, et al. The thermodynamic effect of thermal energy storage on compressed air energy storage system. *Renew Energy* 2013; 50: 227–235.

[5] Chan WL, Chiong MS. A performance study of R717 and R22 as the working fluid for OTEC plant. In: *IOP Conference Series: Earth and Environmental Science*. Institute of Physics, 2023. Epub ahead of print 2023. DOI: 10.1088/1755-1315/1143/1/012018.

[6] Bao J, Zhao L. A review of working fluid and expander selections for organic Rankine cycle. *Renewable and Sustainable Energy Reviews* 2013; 24: 325–342.

[7] Wang HX, Lei B, Wu YT, et al. Regulation strategies and optimizations of the expander and pump in organic Rankine cycle under off-design conditions. *Appl Therm Eng*; 259. Epub ahead of print 15 January 2025. DOI: 10.1016/j.applthermaleng.2024.124807.

[8] Gungor U, Hosoz M. Performance comparison of a mobile air conditioning system using an orifice tube as an expansion device for R1234yf and R134a. *Sci Technol Built Environ* 2024; 30: 588–598.

[9] Fatigati F, Coletta A, Di Bartolomeo M, et al. The dynamic behaviour of ORC-based power units fed by exhaust gases of internal combustion engines in mobile applications. *Appl Therm Eng*; 240. Epub ahead of print 1 March 2024. DOI: 10.1016/j.applthermaleng.2023.122215.

[10] Alshammari F, Karvountzis-Kontakiotis A, Pesyridis A, et al. Expander technologies for automotive engine organic Rankine cycle applications. *Energies*; 11. Epub ahead of print 2018. DOI: 10.3390/en11071905.

[11] Tocci L, Pal T, Pesmazoglou I, et al. Small scale Organic Rankine Cycle (ORC): A techno-economic review. *Energies*; 10. Epub ahead of print 23 March 2017. DOI: 10.3390/en10040413.

[12] Dumont O, Dickes R, Lemort V. Experimental investigation of four volumetric expanders. In: *Energy Procedia*. Elsevier Ltd, 2017, pp. 859–866.

[13] Alshammari F, Karvountzis-Kontakiotis A, Pesyridis A, et al. Expander technologies for automotive engine organic Rankine cycle applications. *Energies*; 11. Epub ahead of print 2018. DOI: 10.3390/en11071905.

[14] Dixon SL, Hall CA. Axial-Flow Turbines. In: *Fluid Mechanics and Thermodynamics of Turbomachinery*. Elsevier, 2010, pp. 97–141.

[15] Ramchandra Rane S, Bianchi G, Kovačević A, et al. *CFD Analysis of an ORC Vane Expander using OpenFOAM Solver*, https://docs.lib.purdue.edu/icec (2021).

[16] S.L. Dixon, C.A. Hall. *Fluid Mechanics, Thermodynamics of Turbomachinery*. United KIngdom: Butterworth-Heinemann, 2014. Epub ahead of print 2014. DOI: https://doi.org/10.1016/C2011-0-05059-7.

.